Int. J. Electrochem. Sci., 15 **(2020)** 4274 – 4286, doi: 10.20964/2020.05.11

International Journal of ELECTROCHEMICAL SCIENCE
www.electrochemsci.org

Density Functional Theory Investigation of Some Pyridine Dicarboxylic Acids Derivatives as Corrosion Inhibitors

A. T. Hassan[1], R.K. Hussein[2], Mortaga Abou-krisha[3, 4] and Mohamed I Attia[3]*

[1] Department of Basic Science, October High institute of Engineering & Technology - OHI, 2nd neighbourhood. 3rd District. 6th of October, Giza, Egypt.
[2] Department of Physics, College of Science, Imam Mohammad Ibn Saud Islamic University (IMSIU), Riyadh 11623, KSA.
[3] Department of Chemistry, College of Science, Imam Mohammad Ibn Saud Islamic University (IMSIU), Riyadh 11623, KSA.
[4] Department of Chemistry, Faculty of Science, South Valley University, Qena, 83523, Egypt
[*]E-mail: eng_rageh@yahoo.com

Received: 6 January 2020 / *Accepted:* 19 February 2020 / *Published:* 10 April 2020

The corrosion inhibition capability of four pyridine dicarboxylic acids was studied using the density functional theory (DFT) method at 6-311G (d, p) basis set. The molecular and electronic properties were investigated to distinguish the best adsorption efficiency on metal surface among the evaluated compounds, namely 2,3-Pyridine dicarboxylic acid, 2,4-Pyridinedicarboxylic acid, 2,5-Pyridine dicarboxylic acid, and 2,6-Pyridinedicarboxylic acid. The relationship between the quantum chemical parameters and inhibition efficiencies was recorded to remark the potential action as corrosion inhibitors. The results of the calculated reactivity parameters such as energy gap (ΔE), electronegativity (χ), electron affinity (A), global hardness (η), softness (σ), ionization potential (I), the fraction of electrons transferred (ΔN), the electrophilicity (ω), molecular electrostatic potential, Mulliken charge, and optimized geometrical structure all supported the advantages of 2,3-Pyridinedicarboxylic acid as a good inhibitor.

Keywords: Pyridine Dicarboxylic Acids; inhibition efficiency; DFT; quantum chemical parameters.

1. INTRODUCTION

Corrosion is one of the most important phenomena which have been widely researched in the last few decades. Corrosion is defined as the degradation of a metal's surface due to chemical reaction with the surrounding. Several studies have been introduced to explore the optimum methods of coating metal surfaces with organic or inorganic materials as a protection in various media [1–3]. The use of corrosion inhibitors is one of the cheapest and most effective techniques for corrosion prevention.

Inorganic composites specified as chromates, nitrates, oxides, and lanthanides have been utilized as common inhibitors for corrosion. Due to some of its toxic effects, there is a need to replace inorganic compounds by environment-friendly materials [4, 5]. Different organic compounds have been recorded as effective corrosion inhibitors of metal surfaces. The molecular structure and the types of functional groups contained in these organic materials clarified their efficient inhibitor characterizations [6, 7]. Aromatic carboxylic acid and their derivatives were reported as effective inhibitors for metal surfaces, especially for aluminum in alkaline solutions [8–10]. A type of organic inhibitor was studied by Marco et al. to prevent corrosion caused by chloride; the results revealed that poly-carboxylates demonstrated very high efficacy as inhibitors [11]. The two oxygen atoms of the carboxylic group caused the adsorption of carboxylates on steel surface through their delocalized electrical charge and a hydrophobic layer covered in the passive films could be formed by the alkyl carbon chain [12]. Previous studies have shown that the efficiency of inhibition increase and decrease by increasing the amount of -COOH groups and decreasing the number of –OH groups contained in inhibitor molecule, respectively. In particular, carboxylic acids were found to be to be highly efficient as an inhibitor of corrosion for aluminum surfaces [13–17].

Although experimental techniques are very useful in the understanding of inhibition mechanism, they do have some limitations, such as being time consuming and highly costly. Recently, the theoretical approach represented by the DFT method has become a considerable tool in studying the inhibition properties of molecules and inhibitor-surface interactions [18–23]. The concepts of DFT have a huge capability to interpret and predict the inhibition performance of organic and inorganic inhibitors based on the reactivity indexes as well as electronic and molecular properties [24–26].

The objective of the present work is to investigate the inhibition efficiency of four carboxylic acid derivatives (Fig. 1), namely 2,3-Pyridine dicarboxylic acid, 2,4-Pyridine dicarboxylic acid, 2,5-Pyridine dicarboxylic acid, and 2,6-Pyridine Dicarboxylic acid. The DFT means were used to determine the structural quantum parameters of these compounds and classify their inhibition efficiency according to the calculated molecular properties.

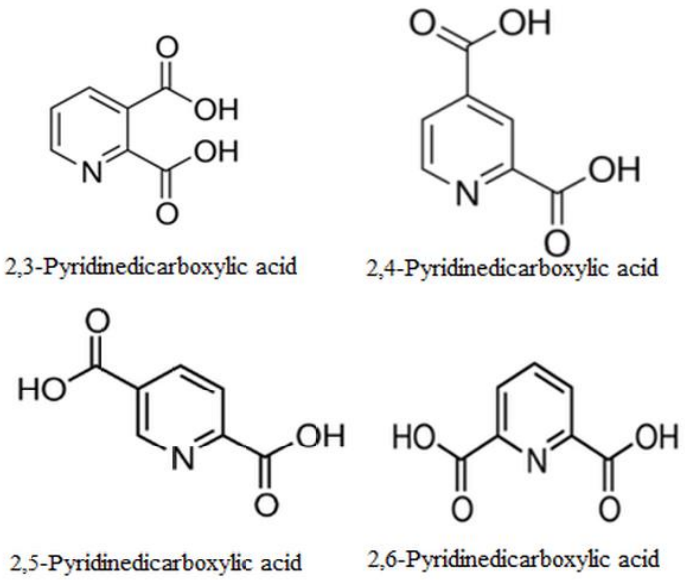

Figure 1. The chemical structures of the studied compounds.

2. COMPUTATIONAL DETAILS

Quantum chemical calculations of the studied pyridine dicarboxylic acid_isomers as corrosion inhibitors were performed using the DFT. Beck's three-parameter exchange function in combination with Lee–Yang–Parr nonlocal correlation functional (B3LYP) and 6-311G (d, p) basis set were used for the calculations [27, 28]. These theoretical parameters were implemented in Gaussian 09 program package [29] to calculate the complete geometry optimizations of all studied compounds.

The investigated electronic structure, molecular properties are used as good descriptors for the inhibition efficiency. The values of the calculated parameters, such as the highest occupied molecular orbital energy (HOMO), the lowest unoccupied molecular orbital energy (LUMO), energy gap $E_{(HOMO–LUMO)}$, ionization potential (I), electron affinity (A), global hardness (η), softness (σ), electronegativity (χ), the fraction of electron transferred (ΔN), and electrophilicity index (ω), are standard evaluations of the potential of corrosion inhibitors. These quantities could be calculated in terms of Koopman's theorem as the following approximations [30, 31].

$$I = -E_{HOMO} \quad (1)$$

$$A = -E_{LUMO} \quad (2)$$

$$\chi = \frac{I+A}{2} = -\frac{(E_{HOMO}+E_{LUMO})}{2} \quad (3)$$

$$\eta = \frac{I-A}{2} = -\frac{(E_{HOMO}-E_{LUMO})}{2} \quad (4)$$

$$\sigma = \frac{1}{\eta} = -\frac{2}{(E_{HOMO}-E_{LUMO})} \quad (5)$$

$$\omega = \frac{\chi^2}{2\eta} \quad (6)$$

$$N_{MAX} = \frac{\chi}{\eta} \quad (7)$$

3. RESULTS AND DISCUSSION

The optimized structures of the studied molecules are shown in Fig. 2. Each structure represents the lowest energy conformer from which the molecular properties and reactivity corresponding to each molecule can be computed. The calculated quantum chemical parameters of the studied compounds are mentioned in Table 1.

E_{HOMO} specifies the molecule's ability to donate electrons. The higher the value of $E_{HOMO,}$ the more the molecule is able to donate electrons, i.e., increasing values of E_{HOMO} will facilitate electron contribution to the metal surface. E_{LUMO} demonstrates the molecule's ability to accept electrons. The filled metal orbits would likely give its electrons to E_{LUMO} with the lower value. As indicated in Table 1, The 2, 3-Pyridinedicarboxylic has the highest inhibition efficiency among the studied compounds because it has both the highest E_{HOMO} and the lowest E_{LUMO} respectively, which indicate good inhibition efficiencies [32].

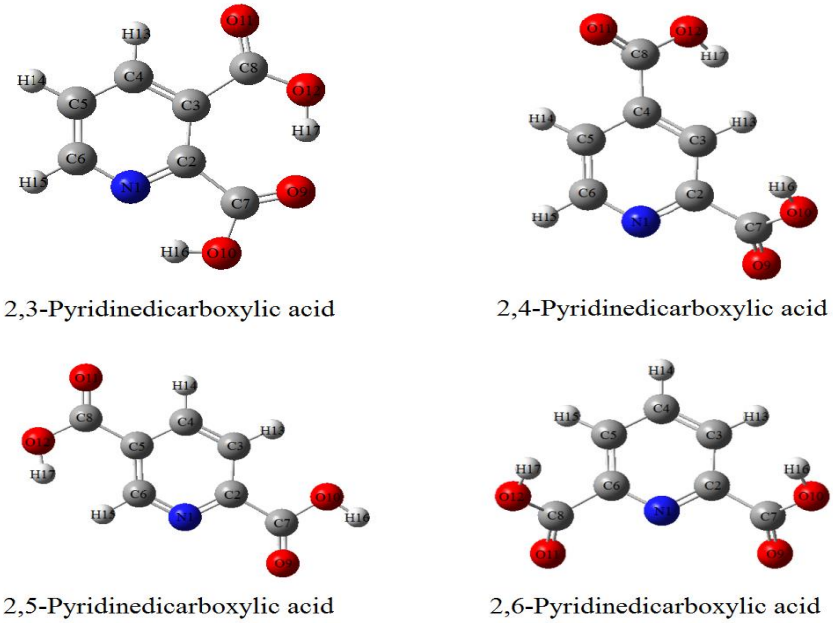

Figure 2. The optimized geometries of the studied compounds.

Table 1. The calculated Quantum chemical descriptors of the studied inhibitors.

Parameter	2,3-Pyridine dicarboxylic acid	2,4-Pyridine dicarboxylic acid	2,5-Pyridine dicarboxylic acid	2,6-Pyridine Dicarboxylic acid
E_{HOMO}	-8.011	-8.114	-8.075	-8.015
E_{LUMO}	-3.100	-2.947	-3.036	-2.544
ΔE	4.911	5.167	5.039	5.471
IP	8.011	8.114	8.075	8.015
EA	3.100	2.947	3.036	2.544
χ	5.556	5.530	5.555	5.279
η	2.456	2.584	2.519	2.736
σ	0.407	0.387	0.397	0.366
ΔN	2.262	2.140	2.205	1.929
ω	6.284	5.917	6.125	5.093

The selectivity of highly efficient inhibitors compounds is associated with its reactivity. The energy difference between HOMO and LUMO orbitals measures the reactivity of inhibitors. Molecules with high-energy difference ΔE (between HOMO and LUMO) indicating low reactivity, while the small values of ΔE representing high reactivity and good inhibition efficiency [33]. The energy difference ΔE of the studied molecules are in the order of 2,6-Pyridinedicarboxylic acid > 2,4-Pyridinedicarboxylic acid > 2,5-Pyridinedicarboxylic acid > 2,3-Pyridinedicarboxylic acid. This result clarified that 2,3-Pyridinedicarboxylic acid with the smallest value of the energy gap has the highest reactivity toward the inhibition reaction. R. H. B. Beda et al studied the properties of caffeine ($C_8H_{10}N_4O_2$) as an inhibitor of aluminum corrosion, the energy gap was found 5.140 eV [34]. Although the 2,3-pyridinedicarboxylic acid ($C_7H_5NO_4$) has two nitrogen atoms less than caffeine, the former has more inhibition effectiveness owing to owning a smaller energy gap 4.911 eV.

Among primary predictors of chemical reactivity of molecules are ionization energy (I) and electron affinity (A). High ionization energy is an index of high stability, while high reactivity of the molecules is due to small ionization energy. As a result, the desired inhibition performance of molecules is associated with high reactivity or small ionization energy [35]. The electron affinity defined as the propensity of a molecule to acquire an electron. Molecules that possess high values of electron affinity are adsorbed strongly onto the metal surface and form a coating protective film [36]. The ability of the inhibitor to accept electrons from the metal surface is increased by increasing the electron affinity. From Table 1, it is clear that 2,3-Pyridinedicarboxylic acid has the smallest value of ionization energy and the highest electron affinity and hence greater inhibition efficiency. The relationship between the ionization energy, electron affinity and between the efficiency of the inhibitors was documented in earlier work. MAB benzoic acid as an aromatic carboxylic acid was synthesized in an experimental and theoretical study by Fanar Hashim et al [37]. The ionization energy and electron affinity of MAB were 11.62 and 4.36 respectively. Our studied molecules are less stable and more energetic with average value 8.05 ionization energy, but MAB has more ability to gain electrons from the metal surface than the studied molecules which have smaller average value 2.90 of electron affinity.

The electronegativity of an atom or molecules is a function of how strongly the attraction of electrons takes place. If an inhibitor has a high value of electronegativity, it means that it has high power for the attraction of electrons from the metal surface [38]. Thus, the inhibitors with greater electronegativity would then have stronger interaction with the metal surface. In Table 1, the electronegativity of the studied molecules follows the order 2,3-Pyridinedicarboxylic acid > 2,5-Pyridinedicarboxylic acid > 2,4-Pyridinedicarboxylic acid > 2,6-Pyridinedicarboxylic acid. Therefore, 2,3-Pyridinedicarboxylic acid has the highest capability to accept electrons and thus a higher capability to bind to metal surfaces. In an analogous study of thiosemicarbazide and tetrazole-based compounds by Abdul-Khalik et al [39], the maximum value of electronegativity was 4.933. By comparing this value with the one in our study we can be certain that the studied dicarboxylic acids have better inhibition properties.

Other remarkable properties to explain the stability and reactivity of molecules are hardness (η) and softness (σ). Chemical hardness implies resistance of atoms to a charge transfer under chemical reaction. The softness defines the ability of molecules to receive electrons. Large energy gap ΔE

corresponds to the harder molecule and small ΔE is indicative of the softer molecule. Hence, the reactive site of the inhibitor strongly adsorbs on the metal surface when the hardness has the smallest value and softness has the highest value [40]. Our work conferred 2,3-Pyridinedicarboxylic acid the highest inhibition efficiency, as it has the lowest hardness value (2.456) and the highest value of global softness (0.407) compared to other compounds. The values of hardness and softness calculated in Beda's work were found to be 2.570 and 0.389 respectively [34]. This gives 2,3-pyridine dicarboxylic acid more privilege of being used as an inhibitor with less hardness and more softness.

The value of ΔN (the number of electrons transferred) indicates the efficiency of corrosion inhibition, resulting from electron donation to the metal surfaces. Findings of a study by Lukovits stated that as long as the value of $\Delta N < 3.6$, the inhibition efficiency increases, as does its ability to donate electrons to metal surfaces [41], i.e., the best inhibitor is associated with the highest value of ΔN. A greater value of ΔN (2.262) was found for 2,3-pyridinedicarboxylic in our results. The inhibition efficiency of indazole derivative [e.g. 1-benzyl-6-nitro-1H-indazole (P1)] has been investigated as a corrosion inhibitor [42]. The presence of many atoms of nitrogen and oxygen in this indazole derivative provides it a large efficiency as an inhibitor. The number of electron transfer for P1 was (2.1356). This result supported the priority of 2, 3-Pyridinedicarboxylic acid as a better inhibitor.

The electrophilicity index ω is a parameter that measures the ability of the inhibitor molecules to accept electrons from metal surfaces. A high value of electrophilicity is described as good capacity to accept electrons from the adjacent metal surfaces. As shown in Table 1, the 2,3-Pyridinedicarboxylic acid reveals the highest value (6.284) of electrophilicity, which evidence the 2, 3-Pyridinedicarboxylic acid is predicted to be the most effective as a corrosion inhibitor as compared to the other molecules. Reactivity descriptors of some thiosemicarbazide derivatives were recently examined [43]. The value of the electrophilicity for Salicylaldehyde thiosemicarbazone (STSC) was 5.481 in confirmation of the high capacity of 2, 3-Pyridinedicarboxylic acid to accept electrons from metal surfaces than thiosemicarbazone.

HOMO provides details about the regions with the most energetic electrons in the molecule. These orbitals are most likely to donate their excess electrons to poor species of electrons. The LUMO is the unoccupied orbital with the lowest energy and provides information about the regions in a molecule with the highest tendency to accept electrons from a species that is rich in electrons. Fig. 3 shows the HOMO and the LUMO surfaces for the studied compounds. The HOMO molecular orbitals are mainly localized on oxygen, nitrogen atoms, and some areas containing carbon atoms, showing that these atoms are the most preferable adsorption sites. In HOMO, the bigger lobes mean the largest contribution to molecular orbitals. O_{11} atom in 2,3-Pyridinedicarboxylic acid has a bigger lobe than the oxygen lobes of the other molecules. This makes 2,3-Pyridinedicarboxylic acid have the highest tendency to offer electrons to the unoccupied orbital of the metal. The LUMO electron densities are distributed over constituent atoms of all the molecules. The widely distributed LUMO electron density around the pyrrole aromatic group, C–COOH bond (carboxyl group), and oxygen atoms is an indication of favorable interactions of the molecules with electron-rich metallic orbitals. The HOMO and LUMO for the studied molecules are quite similar to 5-nitroindazole that was investigated theoretically in a study on the inhibition efficiency of indazole derivatives [44]. The HOMO of 5-nitroindazole was mainly delocalized around the nitrogen and oxygen atoms, LUMO distributed

uniformly around the whole molecule. This result emphasizes the reactivity of molecules as appropriate inhibitors.

The Molecular Electrostatic Potential (MEP) gives information regarding reactive sites for electrophilic and nucleophilic attack. The size, shape, charge density and reactive sites of a broad range of organic materials could be defined clearly by using the electron density isosurface produced by the MEP surface [45]. The MEP map shows different values of electrostatic potential in different colors: red, yellow, green, light blue, and blue. The red and yellow regions on the MEP map are associated with the active electrophilic region, the light blue and blue regions are associated with the active nucleophilic regions. The MEP map of the studied molecules is depicted in Fig. 4. As shown, the more electron-rich regions (red) are located on the oxygen atoms; therefore, oxygen atoms represent the most electrophilic active sites. The nucleophilic reactions occur with hydrogen atoms (blue color). The regions around O_{11}, O_{12} in 2,3-Pyridinedicarboxylic acid have a denser red color than the other molecules. This clarifies the fact that the 2,3-Pyridinedicarboxylic acid is the most predominant toward electrophilic attack and so it has the highest capability of bonding to the metal surface.

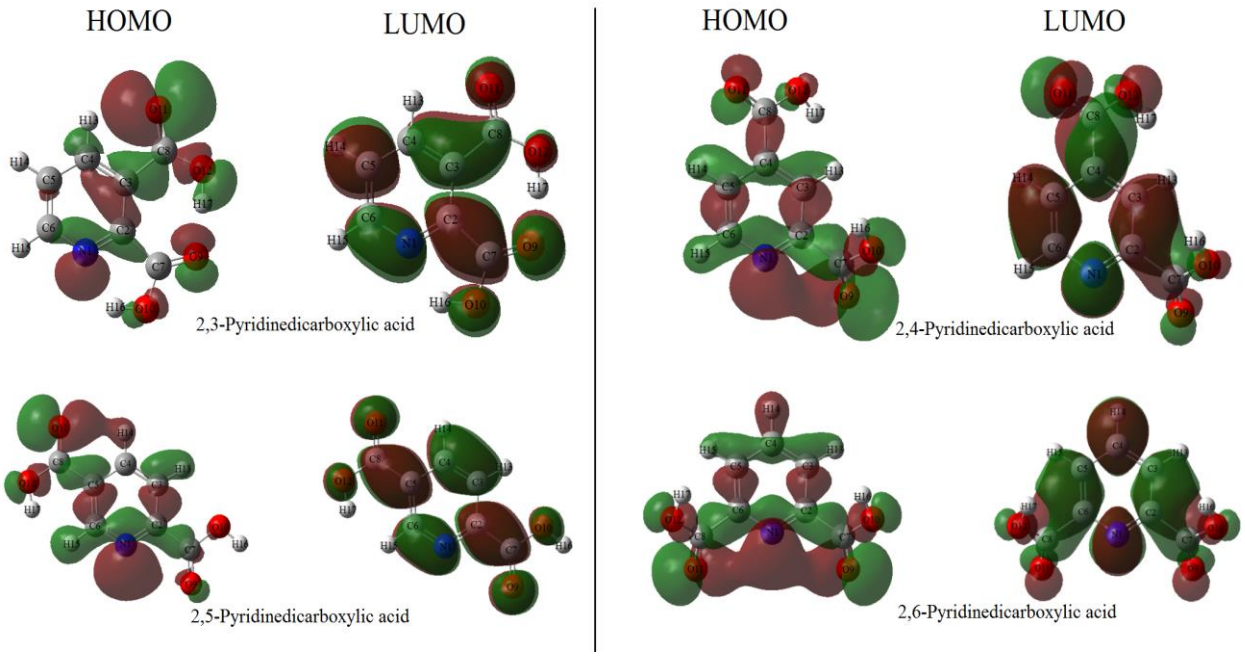

Figure 3. HOMO and LUMO molecular orbitals of the studied compounds.

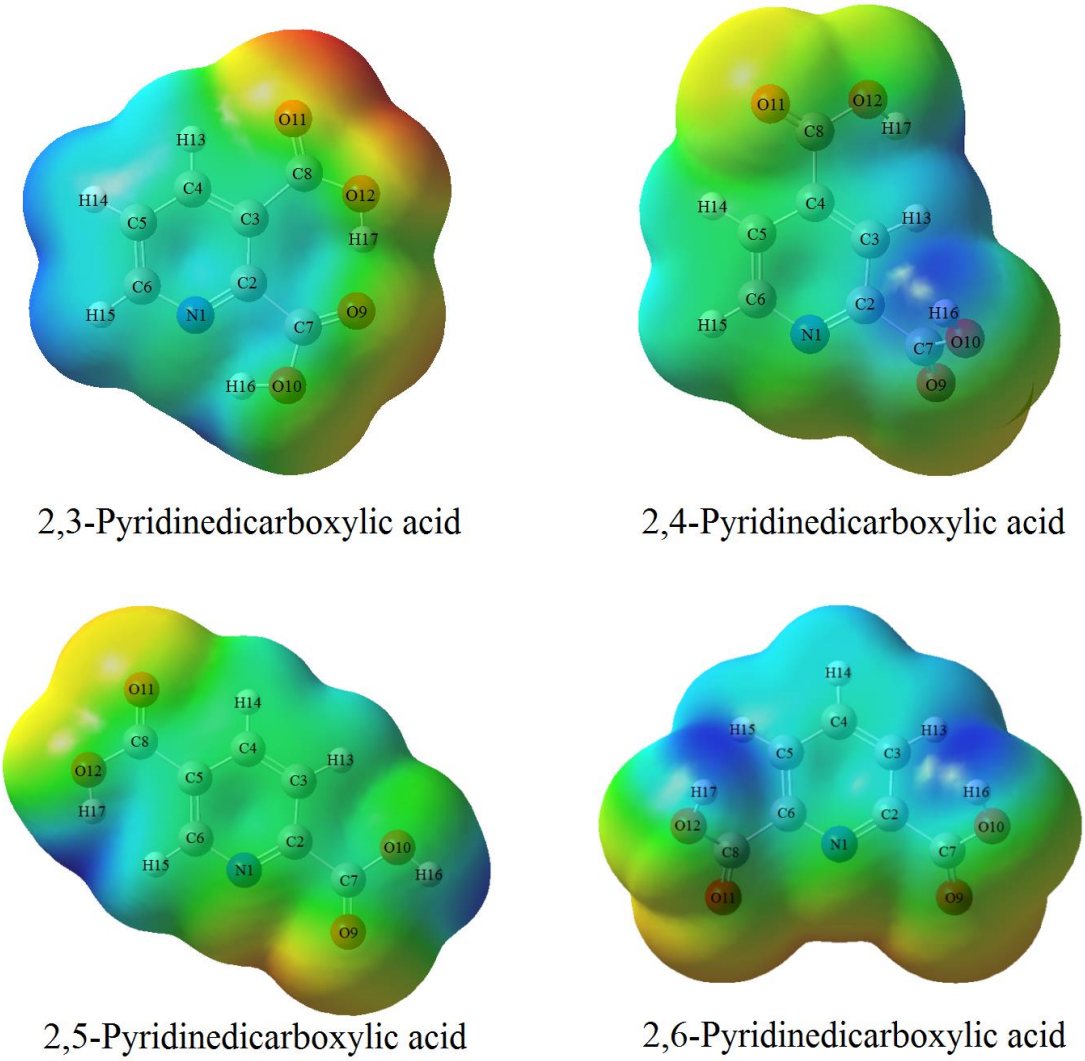

Figure 4. MEP distributions of the investigated inhibitors.

The calculated bond lengths of the studied molecules have been compiled in Table 2. The calculated results agree well with previous experimental and theoretical investigations of the same molecules [46-49]. The salient feature is that the C_2-C_7 bond in 2,3-Pyridinedicarboxylic acid has the longest bond length (the weakest bond). Also, 2,3-Pyridinedicarboxylic acid has the longest C_3-C_8 bond length compared to C_4-C_8, C_5-C_8 and C_6-C_8 in 2,4-Pyridinedicarboxylic acid, 2,5-Pyridinedicarboxylic acid, and 2,6-Pyridinedicarboxylic acid respectively. Since the longer bond lengths are more reactive than the shorter ones and considering that C_2-C_7 and C_x-C_8 connect the pyrrole aromatic group with the two carboxyl group, the longest bond length (weakest bond) C_2-C_7 and C_3-C_8 are entirely compatible with the low-energy gap and high reactivity (previously investigated) of 2,3-Pyridinedicarboxylic acid.

Table 2. Calculated bond lengths of the studied inhibitors.

Parameter	2,3-Pyridine dicarboxylic acid	2,4-Pyridine dicarboxylic acid	2,5-Pyridine dicarboxylic acid	2,6-Pyridine Dicarboxylic acid
N_1-C_2	1.344	1.335	1.336	1.333
N_1-C_6	1.328	1.334	1.329	1.333
C_2-C_3	1.411	1.398	1.399	1.400
C_3-C_4	1.404	1.397	1.388	1.391
C_4-C_5	1.384	1.393	1.396	1.390
C_5-C_6	1.392	1.393	1.401	1.400
C_7-O_9	1.216	1.194	1.200	1.193
C_7-O_{10}	1.320	1.199	1.358	1.363
C_8-O_{11}	1.208	1.199	1.201	1.193
C_8-O_{12}	1.318	1.356	1.354	1.363
O_{10}-H_{16}	0.986	0.966	0.969	0.956
O_{12}-H_{17}	0.966	0.965	0.964	0.956
C_2-C_7	1.522	1.515	1.508	1.517
C_3-C_8	1.541	-------	-------	-------
C_4-C_8	-------	1.506	-------	-------
C_5-C_8	-------	-------	1.504	-------
C_6-C_8	-------	-------	-------	1.517

The planar structure of the inhibitor fragments plays a significant part in the adsorption over the metal surface. Previous studies have shown that molecules with planar geometries are favored in the inhibition reaction than less planar geometries compounds [50]. This is shown by the fact that a planar structure tends to have the majority of its atoms adsorbed over the metal surface than less planar structures. Therefore, inhibitor with planar geometry is the most favored in corrosion inhibitors than non-planar geometry. In this study, dihedral angles analysis was applied to determine the flatness of the studied geometrical structures. Six angle configurations have been inspected, as depicted in Table 3. The computed bond angles of 2,3-Pyridine dicarboxylic acid demonstrated good consistency with that was reported in preceding work [51]. The calculated geometries showed that all structures are nearly planar with the exception of the hydrogen atoms of 2,4-Pyridinedicarboxylic acid and 2,6-Pyridinedicarboxylic acid. The values of the six angles for 2,3-Pyridinedicarboxylic acid and 2,5-Pyridinedicarboxylic acid are close to 0° and 180° respectively, clarifying that they are more planar in structure. The structure of studied Carboxylic Acids describes good planar geometries comparable to the highly planar geometries of quinoline derivatives that categorized as effective corrosion inhibitors [52].

Table 3. The calculated selected dihedral angles of the studied inhibitors.

Parameter	2,3-Pyridine dicarboxylic acid	2,4-Pyridine dicarboxylic acid	2,5-Pyridine dicarboxylic acid	2,6-Pyridine Dicarboxylic acid
N_1-C_2-C_7-O_{10}	-0.00913	-133.152	179.989	-136.883
C_2-C_7-O_{10}-H_{16}	0.00135	11.987	179.998	10.625
C_3-C_2-C_7-O_9	-0.01121	-128.143	179.988	-132.061
C-C-C_8-O_{12}	0.04339	29.890	-179.895	-45.852
C-C-O_{12}-H_{17}	-0.03002	10.158	0.06014	-10.669
C-C-C_8-O_{11}	0.02670	28.299	0.1298	132.069

The calculated Mulliken atomic charges for the optimized structures are presented in Table 4. Multiple researchers have supported the fact that the existence of negatively charged heteroatoms enhances the ability of adsorption on metal surfaces via donor-acceptor mechanisms [53, 54]. The electronegative atoms had a major impact on the inhibition activity in the interaction between the inhibitor molecule and the metal surface. The negative charges on both oxygen and some carbon atoms indicate that these atoms prefer to give electrons to surface atoms and form reactive sites for metal surface adsorption. The highest negative charges are located on the O_9, O_{11}, and O_{12} in 2,3-Pyridinedicarboxylic acid. Likewise, N1 in 2,3-Pyridinedicarboxylic acid has the only negative charge among nitrogen atoms in other compounds. Therefore, N_1, O_9, O_{11}, and O_{12} are a powerful structural characteristic that strengthens the inhibition potential for 2,3-Pyridinedicarboxylic acid. On the other hand, positive charges are required for an efficient inhibitor to balance and counteract the negative charges accumulated on metal surface atoms. The high positive charge makes it easier to accept electrons from metal surfaces to the unoccupied orbital of the positive charge atom. All hydrogen atoms represent acceptor sites, as they carry positive charges; also, some carbons bear positive charge and are considered active adsorption sites. The C_3, H_{16}, and H_{17} atoms in 2,3-Pyridinedicarboxylic acid are the most electron-deficient in all the structures, owing to their highest positive charges.

Table 3. The calculated Mulliken atomic charges on the atoms of the four studied compounds.

Parameter	2,3-Pyridine dicarboxylic acid	2,4-Pyridine dicarboxylic acid	2,5-Pyridine dicarboxylic acid	2,6-Pyridine Dicarboxylic acid
N_1	-0.034	0.088	0.067	0.168
C_2	-1.256	-0.586	-0.665	-0.151
C_3	1.978	0.296	0.264	0.422
C_4	-0.483	0.853	-0.647	-0.861
C5	-0.276	-0.727	0.907	0.422
C_6	0.034	0.049	-0.399	-0.150
C_7	-0.294	-0.357	0.232	-0.132
C_8	-0.051	-0.035	-0.135	-0.132
O_9	-0.357	-0.215	-0.249	-0.222

O_{10}	-0.129	-0.135	-0.192	-0.136
O_{11}	-0.279	-0.235	-0.253	-0.222
O_{12}	-0.277	-0.122	-0.130	-0.136
H_{13}	0.241	0.222	0.269	0.240
H_{14}	0.200	0.216	0.228	0.193
H_{15}	0.218	0.220	0.160	0.240
H_{16}	0.329	0.236	0.306	0.230
H_{17}	0.436	0.234	0.235	0.230

4. CONCLUSIONS

The geometric and electronic properties of pyridine dicarboxylic acids derivatives were investigated for the selectivity of highest efficient characterizations used in inhibition of metal surfaces. DFT calculations at B3LYP/6-31G (d,p) model were used to predict the quantum chemical parameters associated to inhibition efficiency. This work showed excellent inhibition efficiency of the 2, 3-pyridinedicarboxylic acid. The calculated electronic and molecular parameters like E_{HOMO}, E_{LUMO}, energy gap, electronegativity (χ), global hardness (η), softness (σ), the fraction of electrons transferred (ΔN), the electrophilicity (ω), molecular electrostatic potential, mulliken charge have been found that the order of inhibition efficiency of the inhibitors studied is: 2, 3-Pyridinedicarboxylic acid > 2, 5-Pyridinedicarboxylic acid > 2, 4-Pyridinedicarboxylic acid >2, 6-Pyridinedicarboxylic acid.

References

1. T.P. Chou, C. Chandrasekaran, S.J. Limmer, S. Seraji, Y. Wu, M.J. Forbess, C. Nguyen and G.Z. Cao, *J. Non-Cryst. Solids*, 290 (2001) 153.
2. W. Al Zoubi and Y.G. Ko, *Sci. Rep.,* 8 (2018)10925.
3. B. Fotovvati, N. Namdari and A. Dehghanghadikolaei, *J. Manuf. Mater. Process,* 3 (2019) 28.
4. C. Chai, Y. Xu, S. Shi, X. Zhao, Y. Wu, Y. Xu and L. Zhang, *RSC Adv., 8* (2018) 24970.
5. M. Shahid*, Adv. Nat. Sci.: Nanosci. Nanotechnol.,* 2 (2011) 043001.
6. A. Singh, K. Ansari, M. Quraishi and H. Lgaz, *Materials,* 12 (2018) 17.
7. A.A. Al-Suhybani, Y.H. Sultan and W.A. Hamid, *Materialwiss. Werkstofftech.,* 22 (1991) 301.
8. A.R. Madram, F. Shokri, M.R. Sovizi and H. Kalhor, *Electrochim. Acta*, 34 (2016) 395.
9. M.N. Moussa, M.M. El-Tagoury, A.A. Radi and S.M.Hassan, *Anti-Corros. Methods Mater.,* 37 (1990) 4.
10. I. Milošev, T. Bakarič, S. Zanna, A. Seyeux, P. Rodič, M. Poberžnik, F. Chiter, P. Cornette, D. Costa, A. Kokalj and P. Marcus*, J. Electrochem. Soc.,* 166 (2019) 131.
11. M. Ormellese, L. Lazzari, S. Goidanich, G. Fumagalli and A. Brenna*, Corros. Sci.,* 51 (2009) 2959.
12. B. Lin and Y. Zuo, *RSC Adv.,* 9 (2019) 7065.
13. J. Wysocka, S. Krakowiak and J. Ryl, *Electrochim. Acta*, 258 (2017) 1463.
14. J. Wysocka, M. Cieslik, S. Krakowiak, and J. Ryl, *Electrochim. Acta*, 289 (2018) 175.
15. P.S.D. Brito and C.A.C. Sequeira, *J. Fuel Cell Sci. Technol.,* 11 (2014) 011008.
16. B. Müller, *Corros. Sci.,* 46 (2004) 159.
17. J. Ryl, M. Brodowski, M. Kowalski, W. Lipinska, P. Niedzialkowski and J. Wysocka, *Materials,* 12 (2019) 3067.

18. H.L. Madkour and I.H. Elshamy, *Int J Ind Chem.,* 7 (2016) 195.
19. I. Ahamad, R. Prasad, E.E. Ebenso and M.A. Quraishi, *Int J Electrochem Sci.,* 7 (2012) 3436.
20. M. Lashkari and M.R. Arshadi, *Chem. Phys.,* 299 (2004) 131.
21. H.R. Albrakaty, A.N. Wazzan and I.B. Obot, *Int J Electrochem Sci.,* 13 (2018) 3535.
22. P.E. Kumar and M. Govindaraju, *Anti-Corros. Methods Mater.,* 65 (2018) 19.
23. S. Hadisaputra, A.A. Purwoko, A. Hakim, L.R.T. Savalas, R. Rahmawati, S. Hamdiani and N. Nuryono, *J. Phys. Conf. Ser.,* 1402 (2019) 055046.
24. V.V. Mehmeti and A.R. Berisha, *Front. Chem.,* 5 (2017) 61.
25. M.M. Kabanda, L.C. Murulana, M. Ozcan, F. Karadag, I. Dehri, I.B. Obot, E. E. Ebenso, *Int J Electrochem Sci.,* 7 (2012) 5035.
26. F. El Hajjaji, M.E. Belghiti, M. Drissi, M. Fahim, R. Salim, B. Hammouti, M. Taleb and A. Nahlé, *Portugaliae Electrochim Acta,* 37 (2019) 23.
27. A.D. Becke, *J. Chem. Phys.,* 98 (1993) 1372.
28. C. Lee, W. Yang and R.G. Parr, *Phys. Rev. B.,* 37 (1988) 785.
29. M.j. Frisch, G.W. Trucks, H.B. Schlegel, G.E. Scuseria, M.A. Robb, J.R. Cheeseman, G. Scalmani, V. Barone, B. Mennucci, G.A. Petersson, H. Nakatsuji, M. Caricato , Li X, H.P. Hratchian, I. zmaylov, J. Bloino, G. Zheng, J.L. Sonnenberg, M. Hada, M. Ehara, K. Toyota, R. Fukuda, J. Hasegawa, M. Ishida, T. Nakajima, Y. Honda, O. Kitao, H. Nakai, T. Vreven, J.A. Montgomery, J.E. Peralta, F. Ogliaro, M. Bearpark, J.J Heyd, E. Brothers, K.N. Kudin, V.N. Staroverov, R. Kobayashi, J. Normand, K. Raghavachari, A. Rendell, J.C. Burant, S.S. Iyengar, J. Tomasi, M. Cossi, N. Rega, J.M. Millam, M. Klene, J.E. Knox, J.B. Cross, V. Bakken, C. Adamo, J. Jaramillo, R. Gomperts, R.E. Stratmann, O. Yazyev, A.J. Austin, R. Cammi, C. Pomelli, J.W. Ochterski, R.L. Martin, K. Morokuma, V.G. Zakrzewski, G.A. Voth, P. Salvador, J.J. Dannenberg, S. Dapprich, A. D. Daniels , Ö Farkas, J.B. Foresman, J.V. Ortiz, J. Cioslowski and D. J. Fox, Gaussian, Inc. Wallingford CT, (2009).
30. P. Perez, R. Contreras, A. Vela and O. Tapia, *Chem. Phys. Lett.,* 169 (2007) 419.
31. P. Geerlings, F. De Proft, W. Langenaeker, *Chem. Rev.,* 103 (2003) 1793.
32. P.M. Niamien, F.K. Essy, A. Trokourey, A. Yapi, H.K. Aka and D. Diabate, *Mater. Chem. Phys.,* 136 (2012) 59.
33. K.R. Ansari and M.A. Quraishi, *Acid. Phys.,* 69 (2015) 322.
34. R.H.B. Beda, P.M. Niamien, E.B. Avo Bilé, and A. Trokourey. *Advances in Chemistry,* 12 (2017) 24.
35. P. Udhayakalaa, T.V. Rajendiranb and S. Gunasekaranc, *Der Pharma Lettre,* 4 (2012), 1285.
36. M.R. Noor El-Din, E.A. Khamis, *J. Surfactants Deterg.,* 17 (2014) 795.
37. F. Hashim, K. Al-Azawi, S.B. Al-Bghdadi, L.M. Shaker and A. Al-Amiery, *Proceedings,* 41 (15) (2019).
38. R.G. Parr, R.G. Pearson, *J. Am. Chem. Soc.,* 105 (1983) 7512.
39. A. Younis, I.M. Ghayad and F. Kandemirli, *Chemistry and Materials Research,* 11 (2019) 28.
40. W. Huang, Y. Tan, B. Chen, J. Dong and X. Wang, *Tribol. Int.,* 36 (2003)163.
41. I. Lukovits, E. Kalman and F. Zucchi, *Corrosion,* 57 (2001) 3.
42. M.M. Abdelahi, H. Elmsellem, M. Benchidmi, N.K. Sebbar, M.A. Belghiti, L. El Ouasif, A.E. Jilalat, Y. Kadmi and E.M. Essassi, *Journal of Materials and Environmental Sciences,* 8 (2017) 1860.
43. H.U. Nwankwo, L.O. Olasunkanmi and E.E. Ebenso, *Sci. Rep.,* 7 (2017) 2436.
44. S. Xu, S. Zhang, L. Guo , L. Feng and B. Tan, *Materials,* 12 (2019) 1339.
45. S. Bharanidharani and P. Myvizhi, *International Journal of Pure and Applied Mathematics,* 119 (2018) 6769.
46. J.L. Naik, B.V. Reddy and N. Prabavathi, *J. Mol. Struct.,* 1100 (2015) 43.

47. J.L. Naik and B.V. Reddy, *IOP Conference Series: Materials Science and Engineering,* 360 (2018) 012028.
48. V.C. TeÂllez, B.S. GaytaÂn, S. BerneÁs and E.G. Vergara, *Acta Cryst.,* 58 (2002) 228.
49. J.R. Xie, V.H.S. Jr and R.E. Allen, *Chem. Phys.,* 322 (2006) 254.
50. F. Bentiss, M. Traisnel, H. Vezin and M. Lagrene´e, *Ind. Eng. Chem. Res.,* 39 (2000) 3732.
51. M. Karabacak, L. Sinha, O. Prasad, S. Bilgili, A.K. Sachan, A.M. Asiri and A. Atac, *J. Mol. Struct.,* 1095 (2015) 100.
52. E.E. Ebenso, M.M. Kabanda, T. Arslan, M. Saracoglu, F. Kandemirli, L.C. Murulana, A.K. Singh, S.K. Shukla, B. Hammouti, K.F. Khaled, M.A. Quraishi, I.B. Obot and N.O. Eddy, *Int J Electrochem Sci.,* 7 (2012) 5643.
53. M. Beytur, Z.T. Irak, S. Manap and H. Yüksek, *Heliyon*, 5 (2019) e01809.
54. Z. El Adnani, M. Mcharfi, M. Sfaira, M. Benzakour, A.T. Benjelloun, M. Ebn Touhami, *Corros. Sci.,* 68 (2013) 223.